High-density fabrication of normally closed microfluidic valves by patterned deactivation of oxidized polydimethylsiloxane†

Bobak Mosadegh,[a] Hossein Tavana,[ad] Sasha Cai Lesher-Perez[a] and Shuichi Takayama*[abc]

The use of polydimethylsiloxane (PDMS) in microfluidic devices is extensive in academic research. One of the most fundamental treatments is to expose PDMS to plasma oxidation in order to render its surface temporarily hydrophilic and capable of permanent bonding. Here, we show that changes in the surface chemistry induced by plasma oxidation can spatially be counteracted very cleanly and reliably in a scalable manner by subsequent microcontact printing of residual oligomers from a PDMS stamp. We characterize the surface modifications through contact angle, atomic force microscopy, X-ray photoelectron spectroscopy, and bond-strength measurements. We utilize this approach for negating the bonding of a flexible membrane layer within an elastomeric valve and demonstrate its effectiveness by integration of over one thousand normally closed elastomeric valves within a single substrate. In addition, we demonstrate that surface energy patterning can be used for "open microfluidic" applications that utilize spatial control of surface wetting.

Introduction

Microfluidic devices are utilized for a myriad of applications in chemical assays, cell culture platforms, and diagnostic devices.[1–3] One area of research, aimed to enable accessibility of these devices to a broader range of users, is the use of normally closed elastomeric valves (valves that are in a closed state when no pressure is applied) for embedded functionality in microfluidic devices.[4–7] The normally closed valves in these works function based on the principle that a thin membrane deflects from a substrate in a given region but remains bonded in all other areas. Although this type of valve can be fabricated in glass-based substrates by sandwiching an elastomeric membrane and held together by force, the bonding is prone to leakage and working with etched glass is expensive.[4,7–9] Efficient integration of normally closed valves into microfluidic devices that are comprised solely of PDMS would be very useful due to the low cost and widespread use of this material for microfluidic applications. Currently, normally closed elastomeric valves are incorporated in PDMS devices using multi-layer soft-lithographic methods that involve sandwiching a flexible PDMS membrane between two PDMS layers and keeping it from permanently bonding by use of a passivation layer (i.e. salt/photoresist).[10,11] This method is often limited to the fabrication of a single valve or a small number of valves because controlled deposition and washout of the passivation material become exceedingly difficult for more complex devices containing large numbers of integrated valves.

An alternative method is to block exposure of selected regions of a PDMS surface to plasma[12] or corona[13] treatment, which is used to oxidize the PDMS surface and render it hydrophilic and capable of bonding. Typically selective exposure of a surface to plasma/corona treatment is achieved through a stencil; however, stencils can only be used to generate islands of exposed areas but not the inverse pattern needed for the fabrication of normally closed valves.[14–17] One method to achieve patterned non-oxidized islands is to place a PDMS stamp containing extruding features that correspond to desired regions.[5] However, this is only effective for small areas that allow sufficient penetration of plasma/corona under the stamp features and therefore is not applicable for devices with many valves.

Therefore we developed a method to efficiently generate patterns of non-bonding islands on a PDMS surface by use of PDMS oligomers to conceal the surface effects of plasma oxidation in selective areas. Transfer of residual PDMS oligomers during microcontact printing of PDMS stamps has been used to modify the surface energy of various substrates.[18–23] However, the effect of these oligomers on oxidized PDMS surface energy and its binding capability has not been investigated. We show that these oligomers can inhibit bonding between two oxidized PDMS surfaces at the microscale and in a scalable fashion. Utility of this surface modification method is demonstrated through high-density fabrication of normally closed elastomeric valves and surface wettability patterning.

Experimental section

All PDMS materials were made from PDMS prepolymer and curing agent (Sylgard 184, Dow Corning Co., Midland, MI) at a 10 : 1 ratio. PDMS stamps were molded against master molds made by standard photolithography using the negative-photoresist SU-8 (MicroChem Co., Newton, MA). The master molds

[a]Department of Biomedical Engineering, University of Michigan, 2200 Bonisteel Blvd., Ann Arbor, Michigan, 48109-2099, USA. E-mail: takayama@umich.edu
[b]Macromolecular Science and Engineering Center, University of Michigan, 2300 Hayward St, Ann Arbor, Michigan, 48109, USA
[c]Division of Nano-Bio and Chemical Engineering WCU Project, UNIST, Ulsan, Republic of Korea
[d]Department of Biomedical Engineering, University of Akron, 260 S. Forge St., Akron, OH 44325-0302, USA
† Electronic supplementary information (ESI) available: Details on contact angle, atomic force microscopy, and X-ray photoelectron spectroscopy measurements. See DOI: 10.1039/c0lc00112k

were silanized in a desiccator for two hours (United Chemical Tech., Bristol, PA) in order to negate bonding of PDMS to the master molds.[24] The heights of all stamp features were 100 μm. Samples within a given experiment (AFM, XPS and bond strength) were all fabricated concurrently and therefore were exposed to the same baking temperature and baking duration. The PDMS molds were cured in a 120 °C oven for at least 30 min. PDMS substrates for contact angle, Atomic Force Microscopy (AFM), and bond strength experiments were cured in 60 °C for at least 4 h. For X-ray photoelectron spectroscopy (XPS) experiments, a 30 μm PDMS membrane was spun onto glass slides. Similarly, the middle-layer membrane was made by spin-coating a 30 μm PDMS layer on a silanized silicon wafer at 1500 rpm for 90 s and then curing in a 120 °C oven for at least 30 min. For contact angle measurements, PDMS surfaces were oxidized by corona treatment (BD-20AC, Electro-Technic Products Inc., Chicago, IL). For all other experiments, PDMS layers were oxidized/bonded together using a plasma etcher in air (SPI Plasma-Prep II, Structure Probe, Inc., West Chester, PA) for 30 s. The threshold pressure for bond strength experiments was determined by the average readings of a 15 psi pressure sensor (Model PX139-005D4V, Omega Eng. Inc., Stamford, CT) and controlled by a 5 psi pressure regulator (Model PRD2-2N1-0, Beswick Eng., Greenland, NH). Pressured air was delivered *via* a tubing to the PDMS substrate that contained a dead-end circular microchannel feature of 100 μm height and 6 mm diameter.

Contact angles were measured using an axisymmetric drop shape analysis-profile (ADSA-P) methodology.[25] An initial drop of water was deposited on the solid surface from above. Then, a motorized syringe was operated to pump the liquid steadily into the drop so that advancing contact angles were obtained. The images of the drop were recorded during the experiment and analyzed by ADSA-P afterwards. Assuming the drop to be axisymmetric and Laplacian, ADSA-P finds the theoretical drop profile that best matches the drop profile extracted from the image of a real drop. From the best match, contact angles are calculated as the slope of the drop profile at the point of contact with the surface.

Results and discussion

We describe the utilization of the transfer of residual PDMS oligomers onto an oxidized PDMS solid surface for the purpose of patterning wettability and bonding regions. It has previously been shown that PDMS oligomers can have a direct effect on the wettability of oxidized PDMS substrates.[26] The generation of wettability patterns provides a visual demonstration of the surface effects induced by the transfer of PDMS oligomers on the oxidized PDMS surface. Wettability patterns are demonstrated in Fig. 1A where a PDMS slab is initially rendered hydrophilic everywhere by plasma oxidation and then patterned with a hydrophobic (native) PDMS stamp consisting of three embedded channel features. During the stamping process, only those regions of the PDMS slab that do not contact the stamp remain hydrophilic (in this case, underneath the channel features). Other areas on the surface that come in contact with the stamp receive a thin layer of unoxidized oligomers and become more hydrophobic. This generates a pattern of surface energy on the PDMS slab as shown in Fig. 1B using three distinct colored solutions coating only the hydrophilic regions. Difference between the surface energy of linear patterns and the neighboring regions provides a pinning force that prevents the contact line of the liquid from spreading beyond these hydrophilic features.[27] From a surface thermodynamic viewpoint, the hydrophilic features have a smaller solid–liquid interfacial tension than their neighboring deactivated areas when exposed to a liquid and are energetically more favorable for the liquid. Surface energy patterning in and of itself is useful for "open microfluidic" applications which utilize different spatial-wettability of a substrate to form fluidic microstructures.[28–30]

We performed contact angle measurements to study surface modifications induced by deposited PDMS oligomers. Contact angles of deionized water were measured on the surfaces of native PDMS, oxidized PDMS, and deactivated (oxidized and then stamped) PDMS. Corona treatment for 20 s decreases the contact angle from 109° on a native PDMS surface (Fig. 1C) to ∼0° on the oxidized surface (Fig. 1D). Upon the stamping treatment of the oxidized PDMS layer, the surface becomes
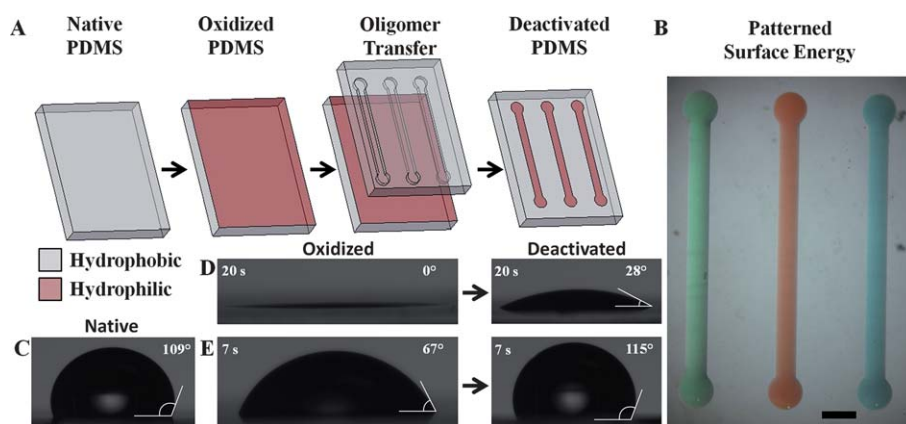

Fig. 1 PDMS deactivation. (A) Scheme for patterning surface energy of an oxidized PDMS layer by a PDMS stamp. (B) Image of the resulting surface energy patterning where three distinct solutions are confined to the hydrophilic areas of the patterned surface. Scale bar: 1.5 mm. Contact angle images and measurements for native PDMS (C), and oxidized and deactivated PDMS for 20 s (D) and 7 s (E) time exposure to corona treatment.

slightly hydrophobic and the contact angle increases to 28°. Our calculations show that this corresponds to a ~14% recovery of surface hydrophobicity (see ESI†).[31,32] Consistently, a shorter treatment of the PDMS surface for 7 s decreases the contact angle only to 67° and upon stamping, the surface converts to a hydrophobic state that exhibits a contact angle of 115° (Fig. 1E). To understand mechanisms responsible for the change in the surface energy due to the stamping process, we

characterized the surface properties of native, oxidized, and deactivated PDMS substrates using AFM and XPS measurements (see ESI†). The oxidized and deactivated surfaces were treated with a plasma etcher for 30 s. For native, oxidized, and deactivated surfaces (all three treatment conditions), the root-mean-square (rms) roughness values from AFM measurements were all less than 1 nm (see ESI†). This indicates that the short duration of oxidation does not induce significant changes in the surface topology[33] and that the difference in the measured contact angles is not due to surface roughness.[25,34]

To examine the effects of oligomers on bonding between oxidized PDMS surfaces, the bond strength between an oxidized PDMS bottom layer and a deactivated, native, or oxidized PDMS top layer was determined by the threshold air pressure needed to separate the two layers (Fig. 2). The pressure was gradually increased using a regulator, pressure readings were taken using an electric pressure transducer, and the separation of layers was visualized under a stereoscope.[35] The deactivated PDMS layer had a significantly lower bonding strength (2.34 PSIG, $p < 0.001$) than the oxidized layer (63.0 PSIG) since the deposited oligomers inhibit the contact of active surface groups on the two PDMS surfaces. Interestingly, the bond strength of the deactivated layer is lower than that of a native layer (3.63 PSIG, $p < 0.05$), suggesting that the PDMS oligomers are uniformly deposited over the entire stamped surface and cover
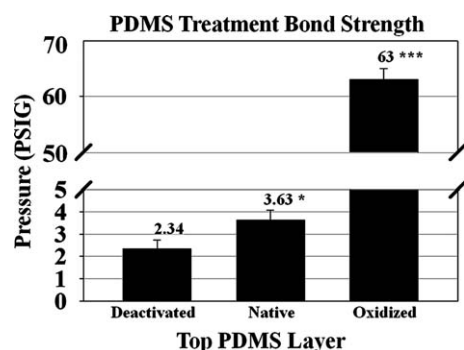

Fig. 2 Bond strength characterization. The threshold pressure required to separate an oxidized PDMS slab from another PDMS layer that is either deactivated (oxidized and then uniformly stamped with PDMS oligomers), native (non-oxidized), or oxidized layer.
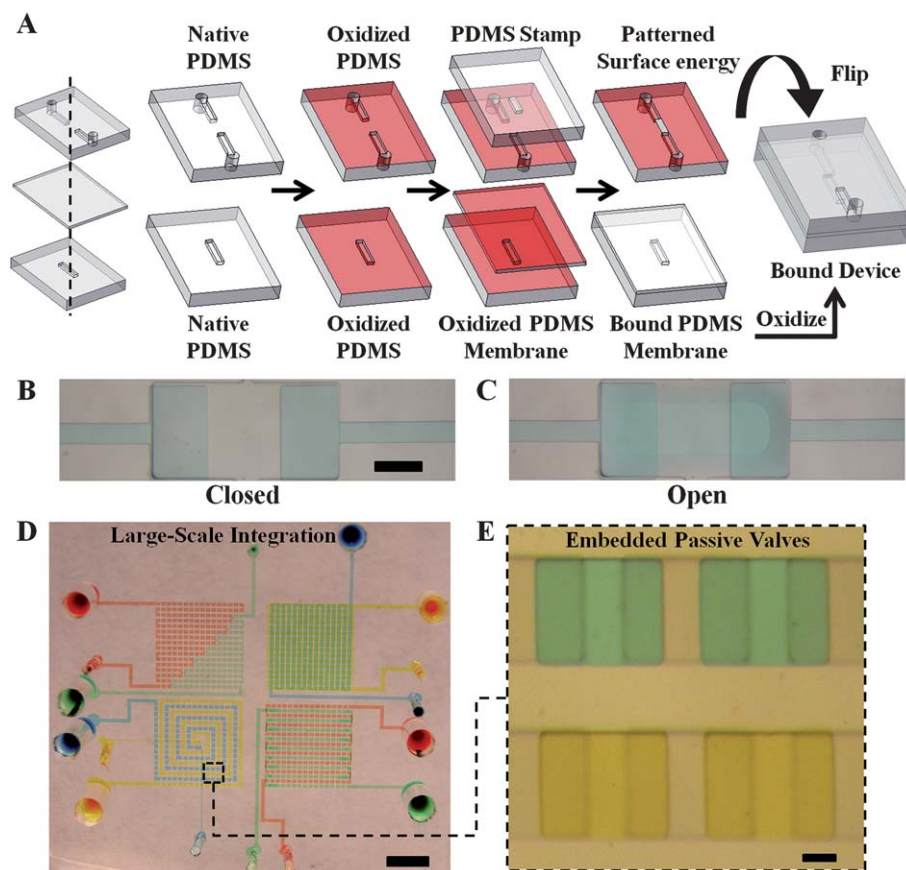

Fig. 3 Integrated elastomeric valves. (A) Scheme for selective bonding of PDMS membrane in an elastomeric valve. (B) Elastomeric valve in a closed position with the membrane flat. Scale bar: 0.25 mm. (C) Elastomeric valve in an open position with the membrane deflected. (D) Picture of large-scale integration of 1010 elastomeric valves on a single substrate. Scale bar: 3 mm. (E) Image of four integrated elastomeric valves in closed position isolating fluids. Scale bar: 125 μm.

active areas of bonding, which would normally have increased the average bond strength between the two layers. The XPS measurements for the proportion of active groups, C–O and C=O that were generated by plasma oxidation, were reduced by over 4% after the deactivation step (see ESI†). This can be attributed to the deposition of PDMS oligomers, which are plentiful in hydrocarbon groups, onto the top surface of the PDMS slab. Coverage of the top surface with these passivating groups makes the surface less hydrophilic and active groups for bonding become hidden.

Efficient blocking of PDMS binding is particularly suited for the fabrication of elastomeric valves, which are an important component to regulate fluids within microfluidic devices.[5,36,37] Normally closed elastomeric valves are of particular interest because they provide embedded functionality with minimal external equipment.[4–11] Fig. 3A shows the fabrication steps for an elastomeric valve consisting of two PDMS feature layers that sandwich a flexible PDMS membrane layer. The top layer contains a disconnected channel, the bottom layer contains a cavity that is located directly under the disconnected region of the top layer, and the middle layer serves as a flexible barrier between the top and bottom layers. After oxidation of the top layer, the disconnect region is deactivated using a PDMS stamp with an extruding feature that matches the disconnect region. The middle membrane layer and bottom layer are oxidized using either a plasma etcher or a corona treating device and all layers are bound together. It should be noted that in order to minimize the time needed to bring layers into contact with each other after plasma treatment, two separate plasma treatment steps should be done (one for the bottom layer to the middle layer and another to bond the top layer). The valve functions by pressurized fluid at one end of the channel, deforming the membrane layer into the cavity region and allowing the fluid to bypass the disconnect region between the channels; the valve closes upon release of the pressure. Fig. 3B and C show the valve in closed and open positions, respectively. This normally closed valving mechanism is a promising component for the development of devices with on-chip fluid regulation.[4–8,10]

We used the above principle in conjunction with the scalability of microcontact printing to enable the large-scale fabrication of normally closed valves (Fig. 3D). The device contains 1010 valves within the equivalent area of a dime, demonstrating the potential for the development of complex devices that utilize numerous integrated normally closed valves for on-chip fluidic control without external actuators. The infusion of four distinct dye solutions demonstrates that all valves were successfully fabricated without any leakage problem. Fig. 3E shows an enlarged region of four integrated valves. Each valve successfully segregates the fluid when in a closed position. The valves are all passive in that they respond automatically to differential pressures (in this case, supplied by a syringe pump). Therefore all valves close automatically when the pressure of the infusing solutions is released. It should be noted that fabricating integrated normally closed valves at high-density is extremely difficult due to the requirement of high-resolution spatial bonding of PDMS. This is an obstacle not present in "normally open" elastomeric valve systems (valves that consist of a control channel that when pressurized deflects a PDMS membrane into a fluid channel sealing it shut), since this type of valve is simply made at the intersection of two channels on either side of a membrane.[38] The ability to segregate liquids automatically may simplify applications that function on the principle of having distinct small volume chambers, such as protein crystallization,[39] digital PCR,[40] and bacterial microcultures.[41] More importantly, normally closed valves are critical components of automated microfluidic flow control circuitry.[4–6,42] The scalable fabrication of such devices requires the ability to efficiently integrate numerous normally closed valves, a technical challenge that this work describes how to overcome in a practical manner.

Conclusions

We have established that residual oligomers from a PDMS stamp can deactivate selected regions of an oxidized PDMS surface and induce changes in surface properties. These changes include rendering hydrophilic surfaces to a more hydrophobic state, which facilitates confining solutions to a pre-defined geometry and negates permanent bonding of two oxidized PDMS substrates by covering up active groups. We demonstrated that this selective bonding technique can be applied to the fabrication of normally closed valves and their large-scale integration using the scalability of microcontact printing. This capability removes a major limitation imposed by practical fabrication issues when designing complex devices with many normally closed valves.

Acknowledgements

References

1 J. West, M. Becker, S. Tombrink and A. Manz, *Anal. Chem.*, 2008, **80**, 4403–4419.
2 A. J. deMello, *Nature*, 2006, **442**, 394–402.
3 D. Janasek, J. Franzke and A. Manz, *Nature*, 2006, **442**, 374–380.
4 D. C. Leslie, C. J. Easley, E. Seker, J. M. Karlinsey, M. Utz, M. R. Begley and J. P. Landers, *Nat. Phys.*, 2009, **5**, 231–235.
5 B. Mosadegh, C.-H. Kuo, Y.-C. Tung, Y. Torisawa, T. Bersano-Begey and S. Takayama, *Nat. Phys.*, 2010, **6**, 433–437.
6 M. Rhee and M. A. Burns, *Lab Chip*, 2009, **9**, 3131–3143.
7 W. H. Grover, R. H. C. Ivester, E. C. Jensen and R. A. Mathies, *Lab Chip*, 2006, **6**, 623–631.
8 D. Irimia and M. Toner, *Lab Chip*, 2006, **6**, 345–352.
9 E. Seker, D. C. Leslie, H. Haj-Hariri, J. P. Landers, M. Utz and M. R. Begley, *Lab Chip*, 2009, **9**, 2691–2697.
10 N. L. Jeon, D. T. Chiu, C. J. Wargo, H. K. Wu, I. S. Choi, J. R. Anderson and G. M. Whitesides, *Biomed. Microdevices*, 2002, **4**, 117–121.
11 J. Y. Baek, J. Y. Park, J. I. Ju, T. S. Lee and S. H. Lee, *J. Micromech. Microeng.*, 2005, **15**, 1015–1020.
12 B. H. Jo, L. M. Van Lerberghe, K. M. Motsegood and D. J. Beebe, *J. Microelectromech. Syst.*, 2000, **9**, 76–81.
13 K. Haubert, T. Drier and D. Beebe, *Lab Chip*, 2006, **6**, 1548–1549.
14 E. Ostuni, R. Kane, C. S. Chen, D. E. Ingber and G. M. Whitesides, *Langmuir*, 2000, **16**, 7811–7819.
15 M. Rhee and M. A. Burns, *Lab Chip*, 2008, **8**, 1365–1373.

16 J. B. Lhoest, E. Detrait, P. van den Bosch de Aguilar and P. Bertrand, *J. Biomed. Mater. Res.*, 1998, **41**, 95–103.

17 A. Tourovskaia, T. Barber, B. T. Wickes, D. Hirdes, B. Grin, D. G. Castner, K. E. Healy and A. Folch, *Langmuir*, 2003, **19**, 4754–4764.

18 Y. K. Kim, G. T. Kim and J. S. Ha, *Adv. Funct. Mater.*, 2007, **17**, 2125–2132.

19 J. A. Wigenius, M. Hamedi and O. Inganas, *Adv. Funct. Mater.*, 2008, **18**, 2563–2571.

20 C. Y. Hui, A. Jagota, Y. Y. Lin and E. J. Kramer, *Langmuir*, 2002, **18**, 1394–1407.

21 R. B. A. Sharpe, D. Burdinski, C. van der Marel, J. A. J. Jansen, J. Huskens, H. J. W. Zandvliet, D. N. Reinhoudt and B. Poelsema, *Langmuir*, 2006, **22**, 5945–5951.

22 C. Thibault, C. Severac, A. F. Mingotaud, C. Vieu and M. Mauzac, *Langmuir*, 2007, **23**, 10706–10714.

23 L. Yang, N. Shirahata, G. Saini, F. Zhang, L. Pei, M. C. Asplund, D. G. Kurth, K. Ariga, K. Sautter, T. Nakanishi, V. Smentkowski and M. R. Linford, *Langmuir*, 2009, **25**, 5674–5683.

24 D. C. Duffy, J. C. McDonald, O. J. A. Schueller and G. M. Whitesides, *Anal. Chem.*, 1998, **70**, 4974–4984.

25 H. Tavana and A. W. Neumann, *Adv. Colloid Interface Sci.*, 2007, **132**, 1–32.

26 J. A. Vickers, M. M. Caulum and C. S. Henry, *Anal. Chem.*, 2006, **78**, 7446–7452.

27 H. Tavana, G. C. Yang, C. M. Yip, D. Appelhans, S. Zschoche, K. Grundke, M. L. Hair and A. W. Neumann, *Langmuir*, 2006, **22**, 628–636.

28 T. Pfohl, F. Mugele, R. Seemann and S. Herminghaus, *ChemPhysChem*, 2003, **4**, 1291–1298.

29 Y. N. Xia, D. Qin and Y. D. Yin, *Curr. Opin. Colloid Interface Sci.*, 2001, **6**, 54–64.

30 T. Ohzono, H. Monobe, K. Shiokawa, M. Fujiwara and Y. Shimizu, *Soft Matter*, 2009, **5**, 4658–4664.

31 H. Tavana, D. Jehnichen, K. Grundke, M. L. Hair and A. W. Neumann, *Adv. Colloid Interface Sci.*, 2007, **134–135**, 236–248.

32 H. Tavana, R. Gitiafroz, M. L. Hair and A. W. Neumann, *J. Adhes.*, 2004, **80**, 705–725.

33 S. M. Hong, S. H. Kim, J. H. Kim and H. I. Hwang, *J. Phys. Conf. Ser.*, 2006, **34**, 656.

34 K. Grundke, *Molecular Interfacial Phenomena of Polymers and Biopolymers*, CRC Press LLC, Boca Raton, 2005.

35 M. A. Eddings, M. A. Johnson and B. K. Gale, *J. Micromech. Microeng.*, 2008, **18**, 067001.

36 S. Pennathur, *Lab Chip*, 2008, **8**, 383–387.

37 G. M. Whitesides, *Nature*, 2006, **442**, 368–373.

38 M. A. Unger, H. P. Chou, T. Thorsen, A. Scherer and S. R. Quake, *Science*, 2000, **288**, 113–116.

39 W. S. Liu, D. L. Chen, W. B. Du, K. P. Nichols and R. F. Ismagilov, *Anal. Chem.*, 2010, **82**, 3276–3282.

40 F. Wang and M. A. Burns, *Biomed. Microdevices*, 2009, **11**, 1071–1080.

41 E. A. Ottesen, J. W. Hong, S. R. Quake and J. R. Leadbetter, *Science*, 2006, **314**, 1464–1467.

42 J. A. Weaver, J. Melin, D. Stark, S. R. Quake and M. A. Horowitz, *Nat. Phys.*, 2010, **6**, 218–223.